Theoretical Mean-Square Displacements for Surface Atoms in Face-Centered Cubic Lattices with Applications to Nickel*

B. C. CLARK AND ROBERT HERMAN
Research Laboratories, General Motors Corporation, Warren, Michigan
AND
R. F. WALLIS
U. S. Naval Research Laboratory, Washington, D. C.
(Received 8 March 1965)

The mean-square displacements of atoms in a face-centered cubic crystal have been calculated as a function of distance from a free surface using the harmonic approximation in the high-temperature limit. The procedure is based on the inversion of the dynamical matrix. Calculations have been made for the (100), (110), and (111) surfaces using a nearest-neighbor central-force model for crystals up to 30 layers thick. The force constants for surface atoms are assumed to be the same as those in the interior. The mean-square displacements increase monotonically from the middle of the crystal to the surface. Anisotropy of the mean-square displacement components is found for the surface atoms in each plane considered. The theoretical results are compared with recent low-energy electron-diffraction data on nickel single crystals.

I. INTRODUCTION

THE development of the low-energy electron-diffraction technique during the last few years has made possible experimental investigations of the configurations and motions of atoms on the surfaces of crystals. Of particular interest is the work of MacRae and Germer[1] on nickel single crystals. They showed that the effective Debye temperature for the scattering of low-energy electrons, which are scattered mainly by the surface atoms, is significantly lower than that of more penetrating high-energy electrons. These results indicate that the mean-square displacements of surface atoms are larger than those of interior atoms.

A calculation of the mean-square displacements of atoms near a free surface of a simple cubic lattice has been made by Rich[2] who assumed nearest-neighbor interactions with equal force constants for the central and noncentral components. Rich found that the mean-square displacement of a surface atom is larger than that of an interior atom by about 15% at very low temperatures and by about 30% near the Debye temperature. This result is consistent with the idea that a surface atom is less tightly bound than an interior atom. Rich also found that an atom in the fifth atomic layer from the surface behaves essentially the same as an atom in an infinite lattice. The nearest-neighbor model has also been treated by Celý[3] and by Corciovei and Berinde.[4]

Maradudin and Melngailis[5] have studied an isotropic simple-cubic lattice with nearest- and next-nearest-neighbor central forces. In addition to the features exhibited by the calculations of Rich, their results indicate that at the surface the mean-square values of displacements parallel and perpendicular to the surface are different. This anisotropy at the surface has also been found by Corciovei and Berinde.[4]

Recently, MacRae[6] has reported experimental results for the (110) plane of nickel which indicate an anisotropy between the perpendicular displacements in the [110] direction and the parallel displacements in the [1$\bar{1}$0] direction. MacRae also observed an anisotropy between the parallel displacements in the [1$\bar{1}$0] and [001] directions.

In the present paper, calculations are reported for the mean-square displacement components of atoms at the (100), (110), and (111) surfaces of a face-centered cubic crystal with nearest-neighbor central forces. The results are obtained in the classical harmonic approximation. Specific application is made to nickel, and a comparison with the experimental results of MacRae is given.

II. GENERAL FORMULATION

The intensity of x rays or electrons which have undergone single scattering by the atoms in a crystal is proportional to the quantity[6,7]

$$|\sum_k \alpha_k f_k e^{i(\mathbf{K}'-\mathbf{K})\cdot\mathbf{r}_k}|^2, \tag{1}$$

where

$$f_k = f_k^0 e^{-M_k}, \tag{2}$$

K and K' are the wave vectors of the incident and scattered radiation, α_k is a transmission factor, and $\mathbf{r}_k$ is the position vector of the kth atom at equilibrium. In Eq. (2), f_k^0 is the atomic scattering factor and e^{-M_k}, which is the square root of the Debye-Waller factor, takes into account the thermal motion of the atom. The quantity M_k is related to the atomic displacement from equilibrium $\mathbf{u}_k$ by

$$M_k = \tfrac{1}{2}\sum_{ij}(K'-K)_i(K'-K)_j\langle u_{ki}u_{kj}\rangle, \tag{3}$$

* A preliminary report of this work was presented at the Chicago Meeting of the American Physical Society, 23–24 October 1964.
[1] A. U. MacRae and L. H. Germer, Phys. Rev. Letters 8, 489 (1962).
[2] M. Rich, Phys. Letters 4, 153 (1963).
[3] J. Celý, Phys. Status Solidi 4, 521 (1964).
[4] A. Corciovei and A. Berinde, J. Phys. Radium 24, 89 (1963).
[5] A. A. Maradudin and J. Melngailis, Phys. Rev. 133, A1188 (1964).
[6] A. U. MacRae, in *International Conference on the Physics and Chemistry of Solid Surfaces, Brown University, 1964* (North-Holland Publishing Company, Amsterdam, 1964); Surface Sci. 2, 522 (1964).
[7] M. Born, Rept. Progr. Phys. 9, 294 (1942).

where i and j refer to the x, y, and z Cartesian coordinates and the angular brackets signify a thermal average over a canonical ensemble.

For elastic scattering, we may write $\mathbf{K}=(2\pi/\lambda)\mathbf{s}$ and $\mathbf{K}'=(2\pi/\lambda)\mathbf{s}'$, where λ is the wavelength of the radiation and $\mathbf{s}$ and $\mathbf{s}'$ are unit vectors in the directions of K and K', respectively. If we denote the angle between $\mathbf{s}'$ and $\mathbf{s}'-\mathbf{s}$ by ψ, then Eq. (3) can be rewritten as

$$M_k=(8\pi^2/\lambda^2)\cos^2\psi\langle(u_{k\Delta\mathbf{s}})^2\rangle, \tag{4}$$

where $u_{k\Delta\mathbf{s}}$ is the component of $\mathbf{u}_k$ in the direction of $\mathbf{s}'-\mathbf{s}$.

A particularly simple case occurs when the vectors $\mathbf{s}$ and $\mathbf{s}'$ make the same glancing angle φ with the scattering plane of interest. Then $\psi=(\pi/2)-\varphi$, the vector $\mathbf{s}'-\mathbf{s}$ is perpendicular to the scattering plane, and

$$M_k=(8\pi^2/\lambda^2)\sin^2\varphi\langle(u_{k\perp})^2\rangle, \tag{5}$$

where $u_{k\perp}$ is the component of $\mathbf{u}_k$ perpendicular to the scattering plane.

If the Debye continuum theory for an isotropic elastic medium is used in the high-temperature limit, the mean square of the ith component of displacement can be expressed as

$$\langle u_{ki}^2\rangle=3h^2T/4\pi^2mk\Theta_D^2, \tag{6}$$

where Θ_D is the Debye temperature. For the actual lattice dynamical case, Eq. (6) serves to define an effective Debye temperature in terms of the mean-square displacement. If one eliminates $\langle(u_{k\Delta s})^2\rangle$ from Eqs. (4) and (6) and substitutes the result for M_k into Eq. (2), one can obtain from Eq. (1) an expression relating the scattered intensity to the Debye temperature Θ_D. By applying this expression to experimental data on the temperature dependence of the peak intensity of a diffraction spot, one can obtain experimental values for the effective Debye temperature. High-energy electrons which penetrate deeply into a crystal should give a Debye temperature characteristic of the mean-square displacements of interior atoms, whereas sufficiently low-energy electrons which are scattered primarily by the surface layer should give a Debye temperature characteristic of surface atoms.

We now turn to the problem of calculating the mean-square displacements in terms of the forces of interaction between the atoms of a crystal. The displacements $\mathbf{u}_k$ are assumed to satisfy the harmonic equations of motion

$$m_k\ddot{u}_{ki}=-\sum_{k'j}\alpha_{ki,k'j}u_{k'j}, \tag{7}$$

where m_k is the mass of atom k and the $\alpha_{ki,k'j}$ are the Hooke's-law force constants. If one makes the transformation

$$v_{ki}=m_k^{1/2}u_{ki}, \tag{8}$$

the equations of motion can be written as

$$\ddot{v}_{ki}=-\sum_{k'j}D_{ki,k'j}v_{k'j}, \tag{9}$$

where the $D_{ki,k'j}$ are the elements of the dynamical matrix and are related to the force constants $\alpha_{ki,k'j}$ by

$$D_{ki,k'j}=\frac{\alpha_{ki,k'j}}{(m_km_{k'})^{1/2}}. \tag{10}$$

It should be noted that the equations of motion given by either Eqs. (7) or (9) are quite general and apply to crystals with free surfaces, impurities, etc.

The calculation of the mean-square displacement matrix $\langle u_{ki}u_{kj}\rangle$ which appears in Eq. (3) can be carried out as indicated by Born.[7] The results can be expressed by the formula

$$\langle u_{ki}u_{kj}\rangle=\sum_p(e_{ki}(p)e_{kj}(p)/m_k)(\bar{\epsilon}_p/\omega_p^2), \tag{11}$$

where $e_{ki}(p)$ is the kith component of the pth eigenvector of the dynamical matrix, ω_p^2 is the corresponding eigenvalue and $\bar{\epsilon}_p$ is the mean energy of the pth normal mode oscillator. If one uses a theorem of matrices discussed by Born,[7] Eq. (11) can be transformed into the form

$$\langle u_{ki}u_{kj}\rangle=(h/2m_k)[D^{-1/2}\coth(hD^{1/2}/2kT)]_{ki,kj}, \tag{12}$$

where D is the dynamical matrix defined by Eq. (10).

In this paper we are particularly concerned with the high-temperature limit $kT>\hbar\omega_L$, where ω_L is the largest normal-mode frequency. Equations (11) and (12) can then be approximated by the following equations, respectively:

$$\langle u_{ki}u_{kj}\rangle\approx(kT/m_k)\sum_p(e_{ki}(p)e_{kj}(p)/\omega_p^2) \tag{13}$$

$$\langle u_{ki}u_{kj}\rangle\approx(kT/m_k)[D^{-1}]_{ki,kj}. \tag{14}$$

For any crystal of reasonable size, the dimensions of D are enormous and provide a formidable barrier to computation. We therefore simplify the situation by considering crystals in the form of parallelepipeds in which free boundary conditions are imposed on one pair of opposite faces and cyclic boundary conditions are imposed on the other two pairs of opposite faces. The shape of the parallelepipeds depends on which free surface is being considered.

In order to facilitate the enumeration of the normal modes, the parallelepipeds were made up of a number of independent, interpenetrating face-centered cubic lattices so that the resulting lattice gave the appearance of either a simple cubic lattice or a deformed simple cubic lattice. The numbers of such independent fcc lattices were two for the (100) surface, one for the (111) surface, and four for the (110) surface. The pairs of linearly independent primitive translation vectors in planes parallel to the surface were taken to be $[(a/2^{1/2},0,0), (0,a/2^{1/2},0)]$ for the (100) surface, $[(a/2^{1/2},0,a/2^{1/2}), (a/2^{1/2},a/2^{1/2},0)]$ for the (111) surface, and $[(-a/2^{3/2}, a/2^{3/2},0), (0,0,a/2^{1/2})]$ for the (110) surface, where a is the nearest-neighbor distance of the face-centered cubic lattice. In each case the crystal lattice is built up by successive translations of the surface plane with the vectors $(0,0,a/2^{1/2})$, $(0,a/2^{1/2},a/2^{1/2})$, and $(a/2^{3/2},$

$a/2^{3/2},0)]$ for the (100), (111), and (110) surfaces, respectively. The displacement components of the atoms for the (100) and (110) surfaces were specified relative to Cartesian axes parallel to the appropriate translation vectors given above. For the (111) surface, however, the displacement components were specified in terms of the unit vectors $(1/3^{1/2}, -1/3^{1/2}, -1/3^{1/2})$, $(1/2^{1/2},1/2^{1/2},0)$ and $(1/6^{1/2}, -1/6^{1/2}, 2/6^{1/2})$.

In carrying out numerical calculations of D^{-1}, it is convenient to consider only real matrices for D. For the (100), (110), and (111) faces of monatomic face-centered cubic crystals the displacements $u_{ki}\equiv u_{lmni}$ in a given normal mode can be chosen to have the form

$$u_{lmni}=(m_0)^{-1/2}\{\sum_{\sigma} T_\sigma(q_1,q_2)\xi_{\sigma ni}(q_1,q_2,p)\}e^{i\omega_p(q_1,q_2)t}, \quad (15)$$

where $i=x$, y, or z; m_0 is the mass of the atoms; p now designates the normal modes corresponding to a given set of values of (q_1,q_2), $\sigma=c$ or s, and

$$T_c(q_1,q_2)=\cos(lq_1+mq_2) \quad (16a)$$

$$T_s(q_1,q_2)=\sin(lq_1+mq_2). \quad (16b)$$

The quantities q_1 and q_2 are wave-vector components introduced by the cyclic boundary conditions. If Eq. (15) is substituted into Eqs. (8) and (9), one sees that the quantities $\xi_{\sigma ni}(q_1,q_2,p)$ constitute the eigenvector components of a reduced dynamical matrix $D(q_1,q_2)$ and satisfy the equation

$$D(q_1,q_2)\xi(q_1,q_2,p) \equiv \begin{Vmatrix} D_{cc}(q_1,q_2) & D_{cs}(q_1,q_2) \\ D_{sc}(q_1,q_2) & D_{ss}(q_1,q_2) \end{Vmatrix} \begin{Vmatrix} \xi_c(q_1,q_2,p) \\ \xi_s(q_1,q_2,p) \end{Vmatrix} = \omega_p^2(q_1,q_2) \begin{Vmatrix} \xi_c(q_1,q_2,p) \\ \xi_s(q_1,q_2,p) \end{Vmatrix}. \quad (17)$$

For a parallelepiped with N^3 atoms, the original dynamical matrix D has dimensions $3N^3\times 3N^3$ whereas the matrices $D(q_1,q_2)$ have dimensions $6N\times 6N$. By utilizing symmetries one can frequently reduce the size of the matrices still further.

Using Eqs. (15), (16), and (17) one may obtain expressions for $\langle u_{lmni}u_{lmnj}\rangle$ analogous to those given by Eqs. (11), (12), (13), and (14). At a general temperature the analog of Eq. (11) is

$$\langle u_{lmni}u_{lmnj}\rangle=\frac{1}{m_0N^2}\sum_{q_1q_2p}\sum_{\sigma\tau}\frac{\bar{\epsilon}_p(q_1,q_2)}{\omega_p^2(q_1,q_2)}T_\sigma(q_1,q_2)T_\tau(q_1,q_2) \times\xi_{\sigma ni}(q_1,q_2,p)\xi_{\tau nj}(q_1,q_2,p), \quad (18)$$

where N is the number of atoms on an edge of the parallelepiped. The analog of Eq. (12) is

$$\langle u_{lmni}u_{lmnj}\rangle=\frac{\hbar}{2m_0N^2}\sum_{q_1q_2}\sum_{\sigma\tau}\{T_\sigma(q_1,q_2)T_\tau(q_1,q_2) \times[D^{-1/2}(q_1,q_2)\coth(\hbar D^{1/2}(q_1,q_2)/2kT)]_{\sigma ni,\tau nj}\}. \quad (19)$$

In the high-temperature limit it is convenient to make use of the following relationships which are valid for the cases under consideration:

$$[D^{-1}(q_1,q_2)]_{cni,cnj}=[D^{-1}(q_1,q_2)]_{sni,snj} \quad (20a)$$

$$[D^{-1}(q_1,q_2)]_{cni,snj}=-[D^{-1}(q_1,q_2)]_{sni,cnj}. \quad (20b)$$

The high-temperature forms of Eqs. (18) and (19) can then be written, respectively, as

$$\langle u_{lmni}u_{lmnj}\rangle=\frac{kT}{m_0N^2}\sum_{q_1q_2p}\frac{\xi_{cni}(q_1,q_2,p)\xi_{cnj}(q_1,q_2,p)}{\omega_p^2(q_1,q_2)} \quad (21)$$

$$\langle u_{lmni}u_{lmnj}\rangle=\frac{kT}{m_0N^2}\sum_{q_1q_2}[D^{-1}(q_1,q_2)]_{cni,cnj}. \quad (22)$$

Our calculations are based primarily on Eq. (22), but some use is made of Eq. (21).

III. APPLICATION TO A FACE-CENTERED CUBIC LATTICE WITH NEAREST-NEIGHBOR CENTRAL INTERACTIONS

We assume that the force $\mathbf{F}_{kk'}$ acting on atom k due to its interaction with atom k' has the form

$$\mathbf{F}_{kk'}=\alpha[(\mathbf{u}_{k'}-\mathbf{u}_k)\cdot(\mathbf{r}_{k'}-\mathbf{r}_k)/|\mathbf{r}_{k'}-\mathbf{r}_k|] \times((\mathbf{r}_{k'}-\mathbf{r}_k)/|\mathbf{r}_{k'}-\mathbf{r}_k|), \quad (23)$$

where $\mathbf{r}_k$ and $\mathbf{r}_{k'}$ are the position vectors for the equilibrium lattice sites of atoms k and k', and α is the Hooke's-law force constant. A face-centered cubic lattice with nearest-neighbor central forces is a stable lattice for $\alpha>0$, whereas simple cubic and body-centered cubic lattices with this type of interaction are unstable.

The equations of motion have been obtained for the nearest-neighbor central-force model of face-centered cubic lattices with free surfaces parallel to (100), (110), and (111) planes. The dynamical matrices $D(q_1,q_2)$ for these three cases are tabulated in the Appendix. All calculations were made in the high-temperature limit. For most sets of (q_1,q_2), $D(q_1,q_2)$ has no zero eigenvalue and the calculation of its inverse presents no essential difficulty; Eq. (22) was then used to obtain the appropriate contribution to the mean-square displacement.

The inverse of the dynamical matrix was found using the Gauss elimination method. The individual inverses for the various q values were then summed as indicated in Eq. (22). As there are a large number of operations necessary in finding the inverse of a matrix the possibility of round-off error must be considered. In view of this the calculation was repeated utilizing double-precision arithmetic in order to check the precision of the calculated inverses. It was found that the diagonal elements of the inverted matrices were accurate to at least six figures. For a few sets of (q_1,q_2) having the form $(n_1\pi,n_2\pi)$, where n_1 and n_2 are integers, $D(q_1,q_2)$ has a zero eigenvalue; consequently, no inverse exists and Eq. (21) was used excluding the term corresponding to the zero eigenvalue. The eigenvalues of $D(q_1,q_2)$ for these special sets of (q_1,q_2) were found by the method

of Wilkenson. The values for the mean-square displacement were then added to the appropriate sum found from Eq. (22). As the contribution to the total mean-square displacement components from these few sets of (q_1,q_2) is quite small, the precision of the calculation is not as crucial as that of the calculation of the inverses. In this calculation at least four significant figures were obtained, which was considered adequate.

An alternative method of eliminating zero eigenvalues is to replace one of the two free surfaces by a fixed surface. Then the inverse of $D(q_1,q_2)$ can be calculated for all sets of (q_1,q_2). A disadvantage of this method is that symmetry operations are lost which are valuable in further reducing the size of the matrices to be inverted. The results presented in this paper were obtained using two free surfaces on opposite faces of the crystal.

The force constant α may be evaluated in a number of ways. One possibility is to seek a value of α which best reproduces the elastic constants c_{11}, c_{12}, and c_{44} or the bulk modulus B as specified by the equations

$$c_{11}=2^{1/2}\alpha/a \tag{24a}$$

$$c_{12}=\alpha/(2^{1/2}a) \tag{24b}$$

$$c_{44}=\alpha/(2^{1/2}a) \tag{24c}$$

$$B=\tfrac{1}{3}(c_{11}+2c_{12})=(2^{3/2}/3a)\alpha, \tag{24d}$$

where a is the nearest-neighbor distance. Equations (24) may be derived by comparing the elastic continuum equations of motion with the continuum limit of Eqs. (7). If dispersion curves determined from neutron scattering are available, α may be chosen to give the best fit between theoretical and experimental dispersion curves. Bearing in mind the ω^2 dependence of the frequency distribution at low frequencies, we see from Eq. (21) that all frequencies contribute approximately uniformly to the mean-square displacement. The procedure of seeking the best fit to the dispersion curves is therefore better than fitting the elastic constants which emphasizes the low-frequency region.

IV. NUMERICAL RESULTS FOR NICKEL

Detailed numerical calculations have been made of the mean-square displacement components of atoms in nickel crystals with free surfaces parallel to the (100), (110), and (111) planes. We have worked in the high-temperature limit of the harmonic approximation with nearest-neighbor central forces. The force constants coupling surface atoms to their neighbors are assumed to be unchanged from those coupling interior atoms to their neighbors.

The value of the nearest-neighbor force constant α was determined in three ways: (a) from the room-temperature value[8] of the elastic constant c_{11} for unmagnetized nickel using Eq. (24a); (b) by fitting the maximum vibrational frequency as determined by

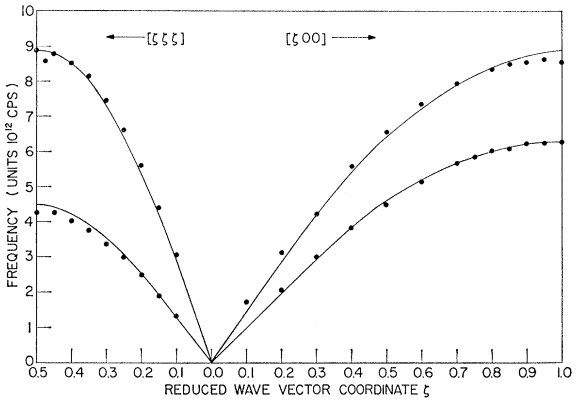

FIG. 1. Phonon dispersion curves for the [100] and [111] directions of propagation in nickel. The theoretical results are indicated by the curves and correspond to case (b) discussed in the text. The experimental results of Birgeneau *et al.* (Ref. 9) are indicated by the solid circles.

Birgeneau *et al.*[9]; (c) by fitting the bulk effective Debye temperature as determined by MacRae and Germer.[1] The phonon dispersion curves were calculated for the bulk nickel crystal for propagation in the [100], [110], and [111] directions. The results for case (b) are presented in Figs. (1) and (2) together with the experimental data for unmagnetized nickel obtained by Birgeneau *et al.*[9] The agreement between the calculated curves and the experimental results is fairly good and indicates that the nearest-neighbor central-force model of nickel with suitably chosen force constant should be reasonably adequate for investigations of lattice vibrational properties of nickel. Case (a) leads to dispersion curves which are about 7% too high at the higher frequencies, while case (c) leads to dispersion curves which are about 9% too low at the higher frequencies. It may be noted that the value of α determined by case (b), $\alpha=3.79\times10^4$ dyn/cm, leads to values of c_{11}, c_{12}, and c_{44} which differ from their room-temperature values[8] by 13, 28, and 11%, respectively.

In Table I are presented the calculated mean-square displacement components in units of kT/α for atoms in successive layers parallel to (100) and (111) free surfaces. In each case the crystals are 20 layers thick with two free surfaces. The components are taken parallel and perpendicular to the respective surfaces. Two mutually perpendicular components parallel to a given surface have the same mean-square displacements because of symmetry. In agreement with previous workers we find that the mean-square displacement components are significantly larger at the surface than in the interior and that the bulk values are very nearly achieved within about five atomic layers from the surface. At each surface the mean-square value of the parallel component is smaller than that of the perpendicular component. This surface anisotropy is similar

[8] J. de Klerk, Proc. Phys. Soc. (London) 73, 337 (1959).

[9] R. J. Birgeneau, J. Cordes, G. Dolling, and A. D. B. Woods, Phys. Rev. 136, A1359 (1964).

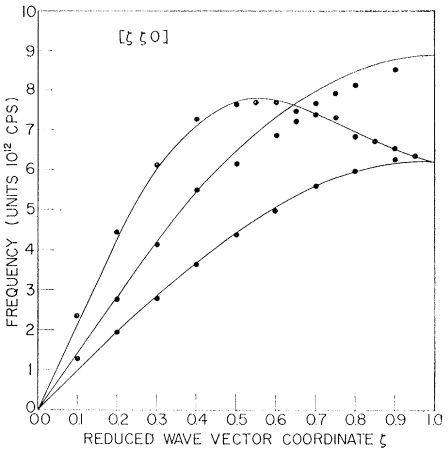

FIG. 2. Phonon dispersion curves for the [110] direction of propagation in nickel. The theoretical results are indicated by the curves and correspond to case (b) discussed in the text. The experimental results of Birgeneau *et al.* (Ref. 9) are indicated by the solid circles.

to that found by Maradudin and Melngailis[5] for a simple cubic lattice.

In Table II are given the calculated mean-square displacement components for atoms in successive layers parallel to a (110) free surface in a crystal 20 layers thick with two free surfaces. The components are taken in the perpendicular direction [110] and the two parallel directions [1$\bar{1}$0] and [001]. The results in Table II exhibit a feature not shown by earlier calculations—namely, a lack of equivalence in the mean-square displacement components in two mutually perpendicular directions parallel to the surface. Otherwise, the qualitative features for the (110) surface are similar to those for the (110) and (111) surfaces.

From low-energy electron-diffraction studies of the (110) surface of nickel MacRae[6] has already obtained experimental evidence for the anisotropies just discussed. Since MacRae presents his results in terms of effective Debye temperatures, we have converted our results to effective Debye temperature using Eq. (6). In Table III we give the calculated values for (110) surface atoms and for atoms at the middle of the crystal for each of the three choices of the force constant

TABLE I. Mean-square displacement components in units of kT/α for atoms in successive layers parallel to (100) and (111) free surfaces of crystals 20 layers thick.

Layer number	(100) ∥	(100) ⊥	(111) ∥	(111) ⊥
1	0.624	0.820	0.532	0.821
2	0.458	0.517	0.445	0.518
3	0.426	0.451	0.425	0.457
4	0.414	0.427	0.416	0.434
5	0.407	0.414	0.411	0.422
6	0.403	0.406	0.408	0.416
7	0.400	0.401	0.405	0.412
8	0.398	0.399	0.403	0.409
9	0.397	0.397	0.402	0.407
10	0.396	0.396	0.402	0.407

TABLE II. Mean-square-displacement components in units of kT/α for atoms in successive layers parallel to (110) free surfaces in a crystal 20 layers thick.

Layer number	[110] (⊥)	[1$\bar{1}$0] (∥)	[001] (∥)
1	0.805	0.643	0.860
2	0.656	0.477	0.490
3	0.494	0.439	0.433
4	0.461	0.422	0.413
5	0.433	0.412	0.404
6	0.420	0.406	0.398
7	0.412	0.401	0.395
8	0.407	0.397	0.393
9	0.403	0.395	0.391
10	0.402	0.394	0.391

α. Also given are values derived from experimental data of MacRae.[6] One sees that choice (a) for α gives Θ_D values which are too high. Choice (b) gives much better agreement with experiment, and choice (c) gives the best agreement. Even for choice (c), however, it is clear that the theoretical results for the [110] and [001] directions are a bit too large.

A question of some interest is how the mean-square displacements of surface atoms depend on the thickness of the crystal. In Fig. 3 are plotted the mean-square displacement components in units of kT/α as a function of crystal thickness for atoms on a (110) surface. In Fig. 4 the ratios of the surface values in the [1$\bar{1}$0] and [001] directions to that in the [110] direction are plotted as a function of thickness. One sees that the ratios are particularly insensitive to the crystal thickness.

It may be noted that the results for the dimensionless mean-square displacements given in Tables I and II and in Figs. 3 and 4 are valid for any face-centered cubic lattice with nearest-neighbor central forces and are not restricted to nickel.

V. DISCUSSION

As in the case of the (100) surface of the simple cubic lattice investigated by previous workers, the mean-square displacement components for the model of a face-centered cubic lattice considered here decrease monotonically from the surface layer toward the interior for each of the (100), (110), and (111) surfaces. After about five atomic layers from the surface, the

TABLE III. Theoretical and experimental effective Debye temperatures associated with mean-square displacement components at the surface and in the bulk of a nickel crystal with a (110) free surface. The experimental data are due to MacRae[6] and the theoretical methods for determining the force constant are given in the text.

Method	[110] (°K)	[1$\bar{1}$0] (°K)	[001] (°K)	Bulk (°K)
(a)	310	348	301	444
(b)	290	325	281	415
(c)	272	306	264	390
expt.	220	330	220	390

TABLE IV. Numbers of bonds broken making angles θ with various displacement directions for the (110) surface.

Angle \ Direction	[110]	[1$\bar{1}$0]	[001]
0°	1	0	0
45°	0	0	4
60°	4	4	0
90°	0	1	1

rate of decrease of the mean-square displacements becomes very small.

The mean-square displacement components for the surface atoms of the (100) and (111) surfaces exhibit an anisotropy analogous to that found by Maradudin and Melngailis[5] in the simple cubic lattice. The parallel component has a smaller mean-square value than the perpendicular component. This is consistent with the qualitative picture that the creation of the free surface leads to a greater reduction of the over-all forces affecting the perpendicular motion than the parallel motion. The (110) surface exhibits a new type of anisotropy—namely, the two mutually perpendicular components which are parallel to the surface do not have the same mean-square value. It is quite clear from an examination of a crystal model that these two directions are not equivalent, so this anisotropy is to be expected and is in fact exhibited by the experimental results of MacRae.[6] If we examine the bonds which are broken in creating the free (110) surface, we may tabulate for a given surface atom the numbers of bonds broken which make various angles θ with a given displacement component. The results are given in Table IV. Since a bond at 90° gives no restoring force

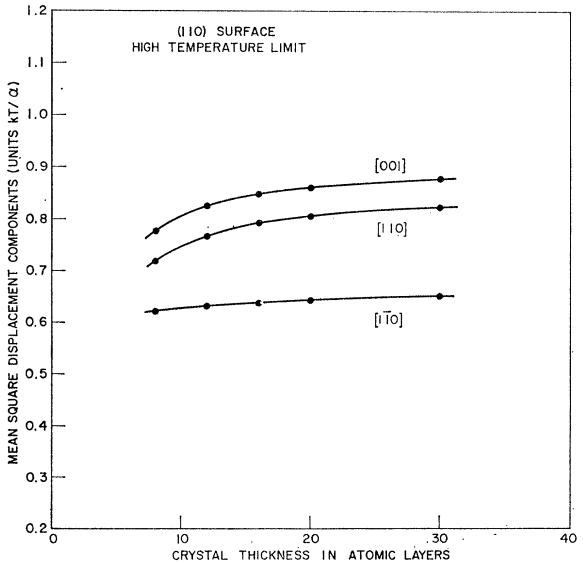

FIG. 3. The mean-square displacement components in units of kT/α plotted as a function of crystal thickness in atomic layers for atoms on the (110) surface. The solid curves are a smooth fit to the calculated points indicated by the solid circles.

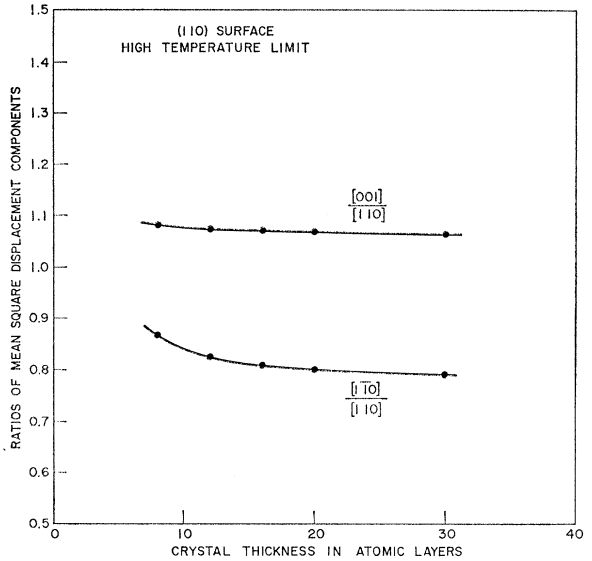

FIG. 4. The ratios of the surface mean-square displacement components in the [1$\bar{1}$0] and [001] directions to that in the [110] direction plotted as functions of crystal thickness in atomic layers for atoms on the (110) surface. The solid curves are a smooth fit to the calculated points indicated by the solid circles.

and a bond at 45° gives a greater effective restoring force than a bond at 60°, it seems reasonable from the numbers in Table IV that both the [110] and [001] displacement components should have larger mean-square values at the (110) surface than the [1$\bar{1}$0] component.

The quantitative comparison between the theoretical and experimental effective Debye temperatures given in Table III requires comment. It is clear that choosing the force constant to fit the elastic constant c_{11} leads to Θ_D values which are too large both at the surface and in the bulk. The reason is that the calculated normal-mode frequencies are too large in the upper frequency range. Choosing the force constant so that the maximum frequency is fitted leads to much better results both for the dispersion curves and the Θ_D values. If the force constant is chosen so that the bulk Θ_D value is fitted exactly, the calculated Θ_D for the [1$\bar{1}$0] direction at the surface is somewhat smaller than the experimental value, while the calculated Θ_D's for the [110] and [001] directions are too large. It is evident that no single choice of the force constant will lead to agreement for all three directions.

There are a number of possible reasons for this discrepancy. First, there is the problem of whether the experimental and theoretical Θ_D's are directly comparable. Experimental factors such as penetration of the electrons beyond the surface layer would tend to invalidate the comparison. From a cursory examination it seems unlikely that this difficulty is responsible for the discrepancy between theory and experiment. Since a detailed analysis of this and other experimental factors is not the province of this paper, we proceed

to discuss several possible shortcomings of our theoretical calculations.

It is possible that the nearest-neighbor central-force model is too simple and that agreement might be improved if additional interactions are included. While the rather good fit which can be obtained to the dispersion curves with the nearest-neighbor model tends to cast doubt that significant improvement can be attained in this way, we are nevertheless carrying out an investigation using a model with nearest- and next-nearest-neighbor central forces together with angle-bending forces involving three consecutive nearest neighbors. This model can of course be applied to other materials than nickel.

A second possibility is that our assumption that the force constants at the surface are the same as in the interior is not correct. It seems likely that appropriate changes in the force constants characterizing the interactions of the surface atoms can lead to significantly better agreement with experiment. This is also under investigation.

Another question which may be raised is how the results for the finite-sized crystals considered here will compare with those for semi-infinite crystals. Although no complete answer can be given, some evidence can be presented. First, the results of Rich[2] and of Maradudin and Melngailis[5] suggest that a crystal which is 20 or more layers thick may be expected to be a reasonable approximation to a crystal of macroscopic size. This conclusion is also indicated by the curves in Figs. (3) and (4). Another piece of evidence concerns the relative magnitudes for the mean-square displacement components associated with three mutually perpendicular directions at the middle of a crystal. For an infinitely large cubic crystal, these three mean-square components should be equal. The lack of equality exhibited by these quantities for the middle layers in the data given in Tables I and II arises from the finite size of the crystals. A possible intuitive estimate of the fractional difference between the mean-square displacements in finite and semi-infinite crystals is $1/N$, where N is the number of layers in the finite crystal. For a crystal 20 layers thick the fractional difference would be 0.05 or 5%. This seems consistent with the trends shown by our calculations. It may also be pointed out that the bulk mean-square displacement which we calculate agrees within about 5% with the bulk value 0.4191 calculated by Maradudin and Flinn[10] using an equation analogous to Eq. (21), but with cyclic boundary conditions along all three axes.

Since nickel is a ferromagnetic element with a Curie temperature of 358°C, one may wonder whether the mean-square displacements are influenced by magnetic effects. MacRae's data for the (110) surface cover the temperature range from 150 to 600°C. There is no indication of anything significant happening at the Curie temperature. De Klerk[8] has measured the elastic constants for both magnetized and unmagnetized nickel at room temperature. The adiabatic constants for the two cases differ by up to 2 or 3%.

As MacRae and Germer[1] have pointed out, at the high temperatures used in obtained the experimental data, anharmonic effects may be appreciable. Application of the results of Maradudin and Flinn[10] to bulk nickel indicates that anharmonic corrections to the mean-square displacement might reach 10–15% at temperatures around 600°C. Since surface atoms have larger mean-square displacements than bulk atoms, the anharmonic corrections may be expected to be larger for the former than the latter. It is indeed possible that the discrepancy between theory and experiment in Table III is at least partly due to the neglect of anharmonic effects.

In summary, the nearest-neighbor central-force model for nickel with unchanged force constants near the surface seems to account for the qualitative features of the surface mean-square displacements as observed in the low-energy electron-diffraction data. Some quantitative discrepancies remain to be resolved.

ACKNOWLEDGMENTS

We wish to thank Dr. A. U. MacRae and Dr. A. D. B. Woods for discussions concerning their experimental work. We also thank Dr. D. C. Gazis and Dr. A. A. Maradudin for helpful discussions, David L. Boice for the use of his computer programs for finding the eigenvalues and eigenvectors and J. T. Oltzyn for helpful discussions regarding the computations.

APPENDIX: REDUCED DYNAMICAL MATRICES FOR THE FACE-CENTERED CUBIC LATTICE WITH NEAREST-NEIGHBOR CENTRAL FORCES

Let $\sigma=c$ or s and $\tau=c$ or s. The reduced dynamical matrices $D_{\sigma\tau}(q_1,q_2)$ can be expressed in terms of 3×3 matrices $d_{ij}=d_{ji}$:

$$D_{\sigma\tau}(q_1,q_2)=\frac{\alpha}{m_0}\begin{Vmatrix} d_{11} & d_{12} & \cdot & \cdot & \cdot & \cdot & \cdot \\ d_{21} & d_{22} & \cdot & \cdot & \cdot & \cdot & \cdot \\ \cdot & \cdot & \cdot & \cdot & \cdot & \cdot & \cdot \\ \cdot & \cdot & \cdot & \cdot & \cdot & \cdot & \cdot \\ \cdot & \cdot & \cdot & \cdot & \cdot & d_{N-1,N-1} & d_{N-1,N} \\ \cdot & \cdot & \cdot & \cdot & \cdot & d_{N,N-1} & d_{N,N} \end{Vmatrix}.$$

[10] A. A. Maradudin and P. A. Flinn, Phys. Rev. **129**, 2529 (1963).

The matrices d_{ij} are expressed in terms of the quantities $c_1=\cos q_1$, $c_2=\cos q_2$, $s_1=\sin q_1$, and $s_2=\sin q_2$. In every case the surface planes are specified by $i=1$ and $i=N$. See Sec. II for the primitive translation vectors used. For (100) surfaces, the 3×3 matrices which make up $D_{cc}(q_1,q_2)$ are

$$d_{ii}=\begin{Vmatrix} 4-2c_1c_2-\delta_{i,1}-\delta_{i,N} & 2s_1s_2 & 0 \\ 2s_1s_2 & 4-2c_1c_2-\delta_{i,1}-\delta_{i,N} & 0 \\ 0 & 0 & 4-2\delta_{i,1}-2\delta_{i,N} \end{Vmatrix},$$

$$d_{i,i+1}=\begin{Vmatrix} -c_1 & 0 & 0 \\ 0 & -c_2 & 0 \\ 0 & 0 & -(c_1+c_2) \end{Vmatrix}$$

$$d_{i,i+j}=\mathbf{0} \quad \text{for} \quad j\geq 2,$$

while those which make up $D_{cs}(q_1,q_2)$ are

$$d_{ii}=\begin{Vmatrix} 0 & 0 & 0 \\ 0 & 0 & 0 \\ 0 & 0 & 0 \end{Vmatrix}, \quad d_{i,i+1}=\begin{Vmatrix} 0 & 0 & -s_1 \\ 0 & 0 & -s_2 \\ -s_1 & -s_2 & 0 \end{Vmatrix}, \quad d_{i,i+j}=\mathbf{0} \text{ for } j\geq 2.$$

$$D_{ss}(c_1,c_2,s_1,s_2)=D_{cc}(c_1,c_2,s_1,s_2), \quad D_{sc}(c_1,c_2,s_1,s_2)=D_{cs}(c_1,\, c_2,\, -s_1,\, -s_2).$$

For (111) surfaces, the 3×3 matrices which make up $D_{cc}(q_1,q_2)$ are

$$d_{ii}=\tfrac{1}{2}\begin{Vmatrix} 4(2-\delta_{i,1}-\delta_{i,N}) & 0 & 0 \\ 0 & -(c_1+4c_2+c_1c_2+s_1s_2-8+\delta_{i,1}+\delta_{i,N}) & -3^{1/2}(c_1-c_1c_2-s_1s_2) \\ 0 & -3^{1/2}(c_1-c_1c_2-s_1s_2) & -(3c_1+3c_1c_2+3s_1s_2-8+\delta_{i,1}+\delta_{i,N}) \end{Vmatrix},$$

$$d_{i,i+1}=\tfrac{1}{6}\begin{Vmatrix} -4(c_1+c_2+1) & -6^{1/2}(c_2-1) & -2^{1/2}(2c_1-c_2-1) \\ -6^{1/2}(c_2-1) & -\tfrac{3}{2}(c_2+1) & \tfrac{1}{2}3^{1/2}(c_2-1) \\ -2^{1/2}(c_1-c_2-1) & \tfrac{1}{2}3^{1/2}(c_2-1) & -\tfrac{1}{2}(4c_1+c_2+1) \end{Vmatrix}, \quad d_{i,i+j}=\mathbf{0} \text{ for } j\geq 2,$$

while those which make up $D_{cs}(q_1,q_2)$ are

$$d_{ii}=\begin{Vmatrix} 0 & 0 & 0 \\ 0 & 0 & 0 \\ 0 & 0 & 0 \end{Vmatrix}, \quad d_{i,i+1}=\tfrac{1}{6}\begin{Vmatrix} 4(s_1+s_2) & 6^{1/2}s_2 & 2^{1/2}(2s_1-s_2) \\ 6^{1/2}s_2 & \tfrac{3}{2}s_2 & -\tfrac{1}{2}3^{1/2}s_2 \\ 2^{1/2}(2s_1-s_2) & -\tfrac{1}{2}3^{1/2}s_2 & \tfrac{1}{2}(4s_1+s_2) \end{Vmatrix}, \quad d_{i,i+j}=\mathbf{0} \text{ for } j\geq 2.$$

$$D_{ss}(c_1,c_2,s_1,s_2)=D_{cc}(c_1,c_2,s_1,s_2), \quad D_{sc}(c_1,c_2,s_1,s_2)=D_{cs}(c_1,\, c_2,\, -s_1,\, -s_2).$$

For (110) surfaces, the 3×3 matrices which make up $D_{cc}(q_1,q_2)$ are

$$d_{ii}=\begin{Vmatrix} 4-\delta_{i,2}-\delta_{i,N-1}-2\delta_{i,1}-2\delta_{i,N} & 0 & 0 \\ 0 & 4-2(c_1^2-s_1^2)-\delta_{i,1}-\delta_{i,N} & 0 \\ 0 & 0 & 4-2\delta_{i,1}-2\delta_{i,N} \end{Vmatrix},$$

$$d_{i,i+1}=\begin{Vmatrix} -c_1c_2 & 0 & 0 \\ 0 & -c_1c_2 & 2^{1/2}s_1s_2 \\ 0 & 2^{1/2}s_1s_2 & -2c_1c_2 \end{Vmatrix}, \quad d_{i,i+2}=\begin{Vmatrix} -1 & 0 & 0 \\ 0 & 0 & 0 \\ 0 & 0 & 0 \end{Vmatrix}, \quad d_{i,i+j}=\mathbf{0} \text{ for } j\geq 3,$$

while those which make up $D_{cs}(q_1q_2)$ are

$$d_{ii}=\mathbf{0}, \quad d_{i,i+1}=\begin{Vmatrix} 0 & -s_1c_2 & -2^{1/2}c_1s_2 \\ -s_1c_2 & 0 & 0 \\ -2^{1/2}c_1s_2 & 0 & 0 \end{Vmatrix}, \quad d_{i,i+j}=\mathbf{0} \text{ for } j\geq 2.$$

$$D_{ss}(c_1,c_2,s_1,s_2)=D_{cc}(c_1,c_2,s_1,s_2), \quad D_{sc}(c_1,c_2,s_1,s_2)=D_{cs}(c_1,\, c_2,\, -s_1,\, -s_2).$$